Copyright © 2008 Tech Science Press SDHM, vol.4, no.2, pp.67-75, 2008

Experimental Assessment of Stress Intensity Factors in Internal Cracks under Mixed-mode Loading

C. Colombo[1], **M. Guagliano**[1,2] **and L. Vergani**[1]

Abstract: With the aim of experimentally assessing the stress intensity factors under mixed-mode loading along a crack front, the case of an internal elliptical crack is analyzed. An experimental test is performed on a three-dimensional photoelastic model made in epoxy resin. This model contains an inner natural crack, created by thermal shock. The crack is inclined in the cylindrical model, loaded with a tensile stress field.

Exploiting the characteristics of the epoxy resin, and using the *stress freezing technique*, it is possible to keep memory of the stresses near to the crack tip, once the specimen is unloaded. The final specimen is cut in slices and K_I, K_{II}, and especially K_{III} are evaluated along the crack front with particular techniques. Comparisons are finally proposed with respect to the analytical solution and the numerical values from a FEM model.

Keyword: Internal elliptical cracks, photoelasticity, mixed-mode loading.

1 Introduction

In many practical cases, the failure of mechanical components is caused by the unstable propagation of internal cracks, pre-existent or nucleated defects for the presence of variable loads. To evaluate the real danger, the significant parameter is the stress intensity factor, divided in K_I, K_{II} and K_{III} in function of the loading mode. Indeed, most of times the knowledge of K_I is sufficient to evaluate the structural integrity of cracked components and structures. However, there are practical cases in which also the other propagation modes must be considered for reliable integrity assessment. For example, internal cracks subjected to rolling contact loads involves both K_I, K_{II}, K_{III} [Guagliano and Vergani (2005)]. It happens in gears, wheels and bearings that are subjected to damage originated in the internal layer of material.

For the determination of the stress intensity factors, it is possible to consider analytical solutions or perform numerical analyses, based on the finite element method or other approaches [Guagliano and Vergani (2005)]. In more complex cases, it is needed also an experimental evaluation to confirm the accuracy of results: for the study of internal defects, these methods can be based on the photoelastic techniques. However also for the application of the photoelastic technique it is necessary to evaluate the grade of accuracy by using it with some cases with a well established theoretical solution.

In this paper, the attention is addressed to a well-known case, being the aim to assess the accuracy of the photoelastic technique in determining the stress intensity factors of an internal crack in a three-dimensional loading case. In this case, indeed, it is possible to have the combined and simultaneous presence of the three loading modes: K_I, K_{II} and K_{III} are different from zero and their values change along the crack front. Besides, the analytical solution of this particular case is known [Kassir and Sih (1966)], and it is suitable to assess the reliability of the experimental results and to evaluate if there are tangible measurement errors.

The analysis deals with an inner elliptical crack, placed in a cylinder and inclined of 45° with respect to the tensile load direction. The radius of the cylinder is sufficient to simulate an infinite body in a tensile field and avoids border effects. In this condition, all the three loading modes are

[1] Dipartimento di Meccanica, Politecnico di Milano, Via La Masa 1, 20156 Milano, ITALY.

[2] Corresponding author: Tel.: +39 022399.8206; Fax.: +39 022399.8202; E-mail: mario.guagliano@polimi.it

present along the crack front; moreover, the crack is in opening conditions, so a good photoelastic signal can be obtained from the experimental tests.

Special care should be taken into account for the experimental determination of K_{III}: there are very few references about this subject. In literature many techniques to experimentally determine the stress intensity factors K_I and K_{II} are described, as [Paris, Picon, Marin, and Cañas (1997)], [Smith and Olaosebikan (1984)], and [Smith, Post and Nicoletto (1983)].

Since the photoelastic technique is mainly based on the analysis of the light crossing transparent specimens, it is immediate to get the fringes in mode I, II and mixed mode I and II loading, but it is not so easy for mode III. Mode III loading occurs in three-dimensional models: to make more general experimental analyses and allow the study of real cases, it is required the evaluation of all the three loading modes. Experimental photoelastic measure analyses for K_{III} was carried out following the *shaving method technique* proposed by [Zhengmei and Ping (1983)].

The comparison of the photoelastic with the analytical solution enables the use of photoelasticity for the analyses on these slices.

2 Photoelastic model and crack generation

The material used for the experimental tests is an epoxy thermosetting resin, whose commercial name is Araldite, with a strong changing of the mechanical characteristics when the temperature is the glass transition one, which is about 120°C. The main mechanical characteristics of this resin are shown in Tab. 1.

Table 1: Characteristics of Araldite below and over glass transition temperature.

	$T < T_{\text{transition}}$	$T > T_{\text{transition}}$
E [MPa]	3500	16
ν	0.35	0.47
σ_R [MPa]	80	2.3
ε_R	0.05	0.15
K_{IC} [MPa$\sqrt{}$mm]	24.43	0.228

The application of the load takes place in the furnace, during a thermal cycle. The particular behavior of the resin allows retaining memory of the applied stress, once the specimen is cooled and unloaded.

To obtain completely natural cracks, the procedure described in [Guagliano, Sangirardi and Vergani (2006)] was followed. Crack is initially created in a cylindrical block of resin from a first casting, imposing a thermal shock trough a heating with an electrical resistance (Voltage =220 V, Power = 25 W, Time = 1 hour), followed by immersion in calm and cold water for a sufficient time (T = 20°C, t = 5 min). In Fig. 1 an elliptical crack with the axes dimensions, measured by the immersion of the cylinder in oil to improve the visibility is shown.

Different trials have been performed to obtain this suitable crack. To perform a reliable photoelastic measurement of K values in the model, the crack should have:

- mainly elliptical shape and good flatness;
- regular borders with sharp tip;
- crack faces next each others, but not in contact.

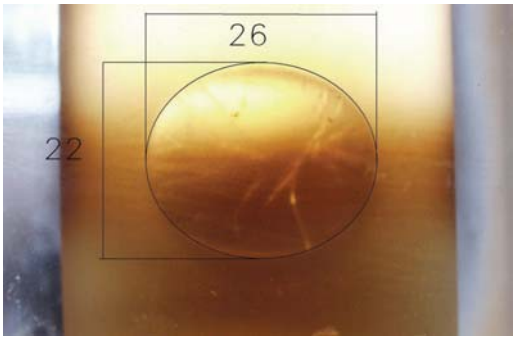

Figure 1: Measure of the crack axes [mm].

Once the suitable crack is obtained, the cylindrical specimen is tool machined in the shape shown in Fig. 2, to ensure a correct placing and inclination of the crack inside the casting of the global model. The chosen angle of inclination is 45° with respect to the axial (identified with the z axis)

or the radial (identified with the y axis) direction of the cylinder, as shown in Fig. 3.

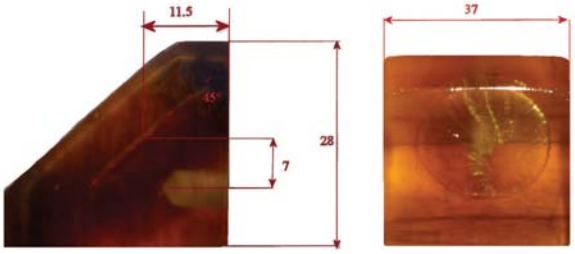

Figure 2: Cracked sub-model cutting and dimensions [mm].

Then the sub-model containing the embedded crack is placed for the second casting, hanging it trough a threaded screw in Araldite, obtained from the first casting.

For this second casting, special care should be taken to avoid the creation of air bubbles near the model containing the crack, which can affect the fringe pattern in the following analysis at the polariscope and therefore the stress intensity factors values.

The raw cylinder, directly obtained from the second casting as shown in Fig. 3.a, is finally cut by a turning machine. Its shape is studied to present two round areas in the upper and lower parts for the further application of the load (see Fig. 3.b).

The global model dimensions were chosen with help of a numerical (Finite Element) model, being the aim to assess if the cylinder radius is large enough to prevent the influence of the cylinder borders on the stress state near the crack front. At the same time the numerical model helped to choose a value of the applied load able to prevent the failure of the model and large enough to produce a good photoelastic signal. The final dimensions of the model are shown in Fig. 3.c.

The FEM model is 3D and was generated using the ABAQUS software. The model is used to simulate the loading conditions, as shown in Fig. 4.a. Boundary conditions and loads are placed on the upper and lower part of the cylinder, according to the experimental test. The model enables to determine the stress state in critical points (see Fig.

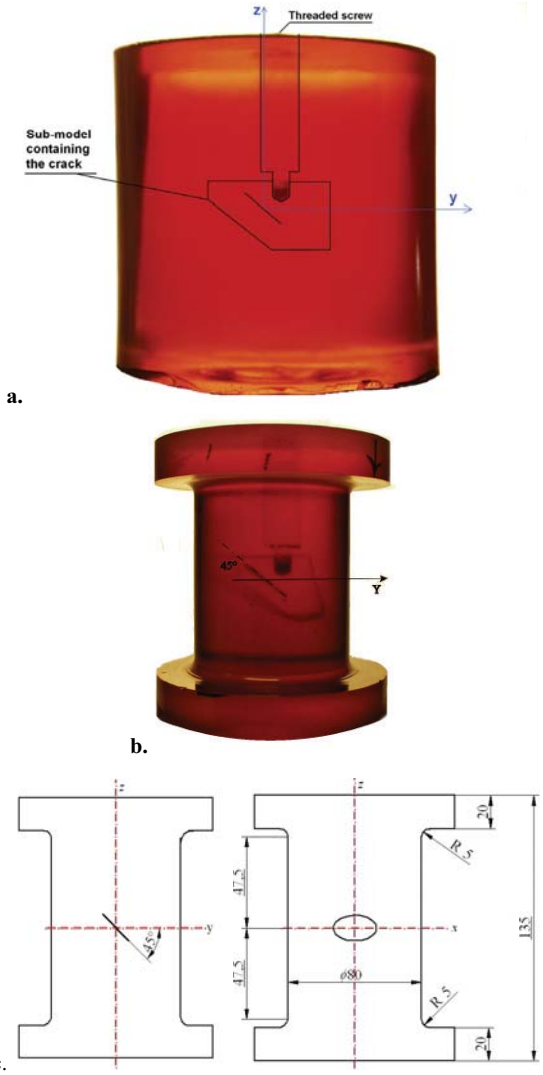

Figure 3: Global cracked model after the second casting (a.), tool-machined (b.) and final dimensions (c.).

4.b) allowing the correct design of the experimental model.

To accurately calculate the stress intensity factors along the crack front a sub-model of the zone around the crack is realized. The displacements of its boundary nodes are imposed from the results of the global model. For this numerical study, the indications included in [Colombo, Guagliano, Vergani (2007)] and [Banks-Sills and Sherman (1992)] are followed. The sub-model with a magnification of the mesh in correspondence of the crack area is shown in Fig. 4.c.

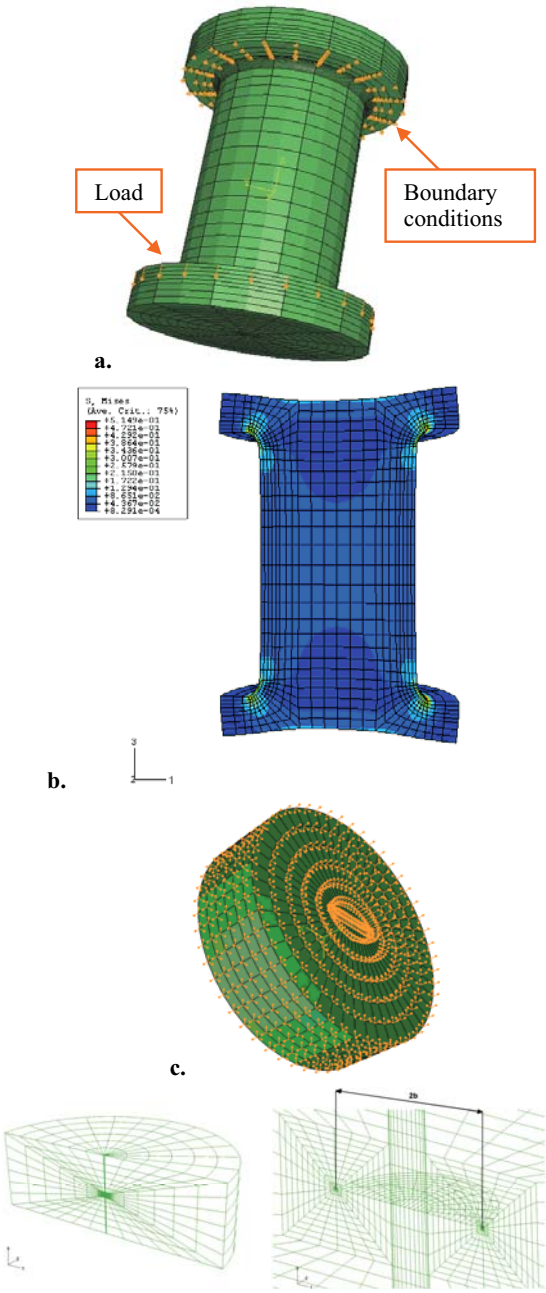

Figure 4: a. FEM model with load and boundary conditions; b. von Mises stress map; c. sub-model of the cracked zone.

According to this numerical study, the load, selected for the experimental test, is P = 295 N. This value results the best compromise between the photoelastic needs and the condition of non-propagation for the crack.

Once the model is ready and the load numerically verified as described, the experimental study can be performed.

Due to the triaxiality of the stress state it is not possible to elaborate the photoelastic signal directly at the polariscope but it is necessary to use the so called *stress freezing* technique. This latter consists in the application of the load in a furnace, during a thermal cycle. In fact, the particular behavior of the resin allows retaining memory of the applied stress, once the specimen is cooled and unloaded. According to this technique, the model of Fig. 3 was loaded in a furnace, like shown in Fig. 5. A loading system was designed and applied to the circular areas at the ending parts of the cylinder [Guagliano, Sangirardi and Vergani (2006)]. The load is constituted of a weight.

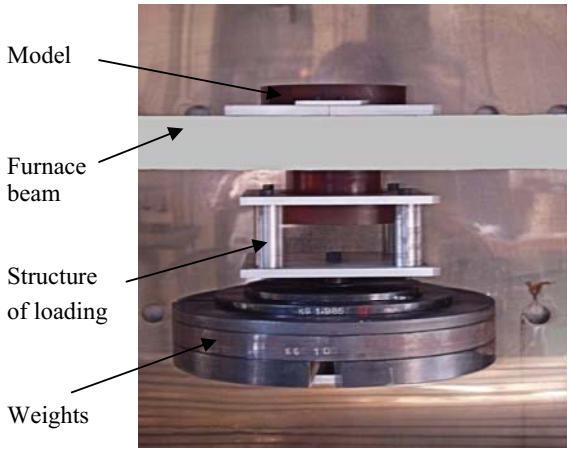

Figure 5: Load application in the furnace.

The observation and the subsequent elaboration of the photoelastic fringes requires to cut thin slices near the crack front zones of interest. The points considered are the ones on the minor (points C and D) and major(points A and B) axes of the crack front, see Fig. 6. The slice with C and D tips is used for K_I and K_{II} evaluation, while slices with A and B tips are used for K_{III} experimental determination.

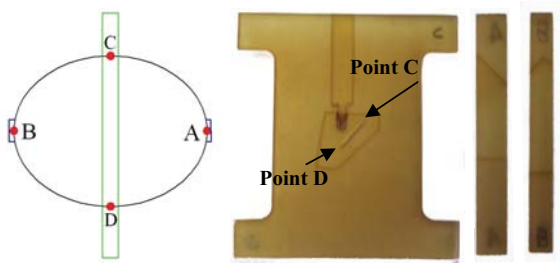

Figure 6: Schematization of slices extraction from the resin model.

3 Experimental results

Analyzing the slice corresponding to C and D points, shown in Fig. 7, it is possible to note a stress concentration in the area of the fillets, and especially near to the crack tips. Fringes around points C and D are analyzed to find K_I and K_{II}. Firstly, white light is used to verify the absence of contact fringes, which means crack in opening conditions. In this case, formulas from fracture mechanics are worthy.

The method, used to determine K values, is described in [Dally and Riley (1991)], and consists of measuring the experimental values of three points in polar coordinates (r, θ), from experimental images taken with photoelastic techniques in monochromatic light.

The equation used to determine the stress intensity values is a non-linear relation in the three unknowns K_I, K_{II} and σ_{0x} (also called T-stress):

$$\left(\frac{Nf_\sigma}{h}\right)^2 = \frac{1}{2\pi r}\left\{[K_I\sin(\vartheta)+2K_{II}\cos(\vartheta)]^2+[K_{II}\sin(\vartheta)]^2\right\} + 2\sigma_{0x}\frac{1}{\sqrt{2\pi r}}\sin\left(\frac{\vartheta}{2}\right)\{K_I\sin(\vartheta)[1+2\cos(\vartheta)]\} + 2\sigma_{0x}\frac{1}{\sqrt{2\pi r}}\sin\left(\frac{\vartheta}{2}\right)\left\{K_I\left[1+2\cos(\vartheta)^2+\cos(\vartheta)\right]\right\}+\sigma_{0x}^2 \quad (1)$$

where N is the fringe order; f_σ = 0.287 N/mm is the photoelastic constant, experimentally measured from a calibration disk; h = 5 mm is the thickness of the analyzed slice.

It is possible to solve Eq. 1 by considering two consecutive fringes $N_1 > N_2$, and measuring r distances along the directions indicated with $\theta = \pi/2$ and $\theta = \pi$, as shown in Fig. 8 for the case of point C. Tab. 2 and 3 show the obtained results in experimental test for the two tips (C and D), included in the slice of Fig.7.

Figure 7: Slice corresponding to C and D points analyzed in monochromatic light.

Table 2: Experimental results in C tip.

Fringe order N_1	3
Fringe order N_2	2
r_1 [mm]	0.560
r_2 [mm]	1.207
r_3 [mm]	1.778
K_I [MPa$\sqrt{}$mm]	0.1330
K_{II} [MPa$\sqrt{}$mm]	-0.1653

For the determination of K_{III} with the photoelastic technique, the used method is proposed in [Zengmei and Ping (1983)], known as *shaving method*. Steps are the following:

- cut of the slices, tangent to the tip to be analyzed and with thickness $t_0 = 2 \div 4$ mm;
- progressive decrease of the thickness in the face opposite to the tip, with steps of

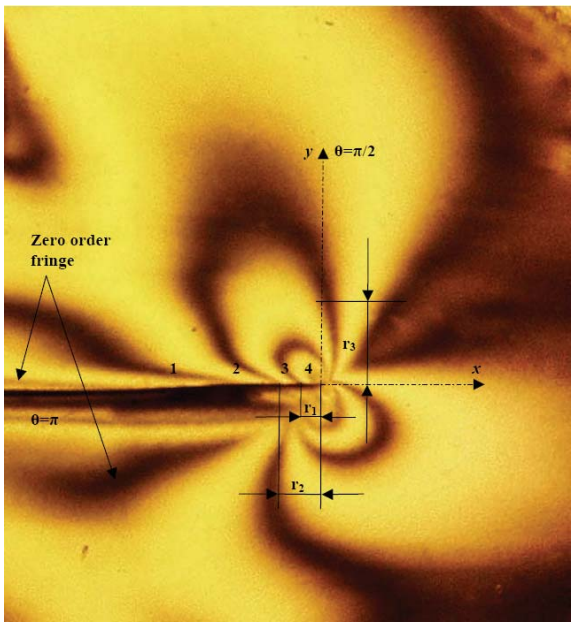

Figure 8: Fringe order identification near to the crack tip (point C).

Table 3: Experimental results in D tip.

Fringe order N_1	4
Fringe order N_2	3
r_1 [mm]	0.360
r_2 [mm]	0.665
r_3 [mm]	0.332
K_I [MPa$\sqrt{}$mm]	0.1235
K_{II} [MPa$\sqrt{}$mm]	0.1603

0.02÷0.2 mm till a thickness of 1 mm is reached. This is the crucial point of the method since it is difficult to obtain regular slices thin enough to give a measurable signal and, at the same time, it is easy to break the slices during the removal of the thickness, due to its limited value. At each step, photoelastic analyses are performed by means of a reflection polariscope combined with a Babinet-Soleil compensator. The values of slice thickness t_i, isoclinic parameter α_{xi} (45°) and fringe order N_{xi} are measured, by observing the slice along x direction, as defined in Fig. 9, for every thickness value.

- determination of the slope q of the straight line, which interpolates the values $(\sqrt{t_i}; N_{xi})$, as is shown in Fig. 10.

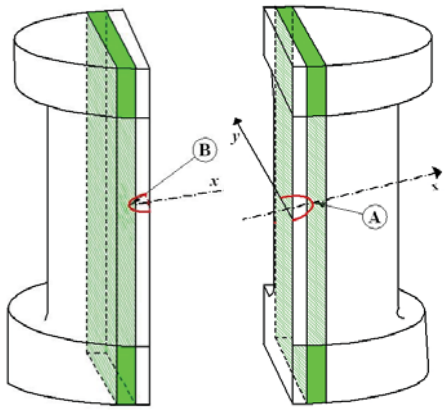

Figure 9: Area of slices extraction from global model.

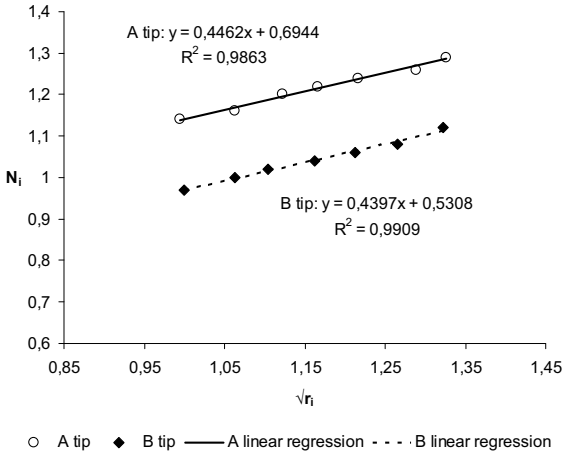

Figure 10: Linear regression to obtain the slope q, for A and B tips.

The relation finally used to calculate K_{III} is:

$$K_{III} = qf\sin(2\alpha_x)\frac{\sqrt{2\pi}}{4} \tag{2}$$

Obtained experimental results are finally presented in Tab. 4, while slices are shown in Fig. 11.

4 Discussion

From the experimental tests it is evident that the applied load was sufficient to obtain a good pho-

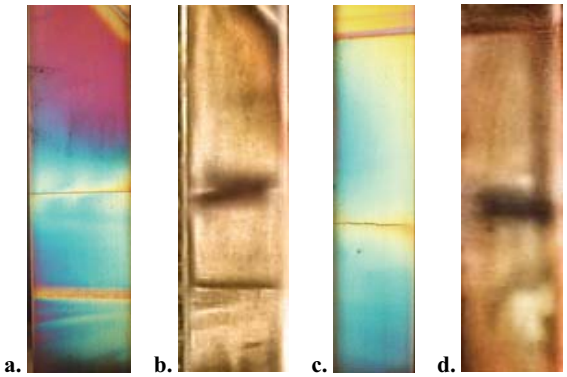

Figure 11: A (a., b.) and B (c., d.) tips in white and monochromatic light.

Table 4: Experimental results in A and B tips.

K_{III}, A [MPa$\sqrt{}$mm]	-0.080
K_{III}, B [MPa$\sqrt{}$mm]	0.079

toelastic signal; the experimental crack is in opening conditions ($K_I > 0$) along all its front, avoiding contact problems in the fringe analysis.

The assessment of the accuracy of the experimental results was performed by comparing them to the analytical and the numerical (FEM) ones. The analytical solution is provided by Kassir and Sih (1996), while the numerical solution was obtained by using the model described in Paragraph 2.

The analytical and numerical results does not show a significant difference, while more pronounced deviation is observed with respect of the experimental results, see Table 5. The most relevant difference is observed at point C.

It is observed that the experimental results always overestimate the stress intensity factors for all the considered points and the loading modes (K_I, K_{II} and K_{III}).

Possible experimental errors are due to the difficulties related to the preparation and the loading of the experimental model (i.e., the stress freezing technique). Due to the symmetry of the problem, K_I should be the same at points C and D, but the experimental values have a difference of 7.1%. This means that the load was probably not perfectly aligned with the crack axis.

The difference of the experimental absolute value of K_{II} between points C and D is about 3%, even if these two values should be equal but with opposite sign. This can be interpreted by considering the irregularities of the model. Experimental values for K_{III} at points A and B are basically the same, except for the sign.

Other sources of measure errors are due to the possible thermal gradient that can influence the stresses, which is not considered in analytical and numerical results.

According to these considerations, experimental results can be however considered sufficiently reliable and confirm the possibility to use the photoelastic technique for the analysis of cracked components under mixed-mode loading conditions.

5 Conclusions

The possibility to use the photoelasticity for determining the stress intensity factors under mixed-mode loading is investigated for the case of a plane internal crack with elliptical shape. The crack is placed in a field of tensile loading and the crack plane is inclined with respect to the load direction. This generates a mixed-mode loading condition, with the combined presence of K_I, K_{II} and K_{III} along the crack front.

A photoelastic test is proposed using a model made in epoxy resin, in which it is placed the embedded crack, naturally obtained by a thermal shock. This allows to perform a three dimensional analysis, using the *stress freezing technique*.

Following conclusions can be drawn, according to the photoelastic results:

- the chosen load for experimental analysis generates a good photoelastic signal for all the considered points along the crack front, but avoiding the instable propagation of the crack;
- K_I, K_{II} and K_{III} are simultaneously present along the crack tip, and values are obtained by photoelastic means;
- experimental evaluations are proposed in correspondence of the points where the ellipse that describes the crack front crosses

Table 5: Comparison between experimental, analytical and numerical solutions.

Point C	K_I	K_{II}
Experimental [MPa$\sqrt{}$mm]	0.1330	-0.1653
Analytical [MPa$\sqrt{}$mm]	0.1185	-0.1492
Numerical [MPa$\sqrt{}$mm]	0.1157	-0.1489
Difference % experimental-analytical	+12.27%	+10.76%
Difference % experimental-numerical	+14.95%	+11.01%

Point D	K_I	K_{II}
Experimental [MPa$\sqrt{}$mm]	0.1235	0.1603
Analytical [MPa$\sqrt{}$mm]	0.1185	0.1492
Numerical [MPa$\sqrt{}$mm]	0.1155	0.1489
Difference % experimental-analytical	+4.18%	+7.46%
Difference % experimental-numerical	+6.9%	+7.65%

	K_{III}, A	K_{III}, B
Experimental [MPa$\sqrt{}$mm]	-0.080	0.079
Analytical [MPa$\sqrt{}$mm]	-0.073	0.073
Numerical [MPa$\sqrt{}$mm]	-0.072	0.072
Difference % experimental-analytical	+9.6%	+8.2%
Difference % experimental-numerical	+11.1%	+9.72%

its minor (points C and D) and major (points A and B) axes. In points C and D there is the mixed presence of K_I and K_{II}, while K_{III} can be evaluated in points A and B. The photoelastic analysis of fringe patterns allows evaluating the stress intensity factors; experimental values are then compared to the numerical and analytical results. The observed differences are mainly related to the experimental difficulties in measuring the photoelastic data.

References

Banks-Sills, L.; Sherman, D. (1992): On the computation of stress intensity factors for three-dimensional geometries by means of the stiffness derivative and J-integral methods. *Int. J. Fracture*, vol. 53, pp. 1-20.

Colombo, C.; Guagliano, M.; Vergani, L. (2007): Numerical determination of stress intensity factors in internal cracks under mixed-mode loading, *Theor. Appl. Fract. Mec*, submitted.

Dally, J.W.; Riley, W.F. (1991): Experimental stress analysis. McGraw-Hill, New York, International Editions, Third Edition.

Guagliano M., Vergani L. (2005): Experimental and numerical analysis of sub-surface cracks in railway wheels, *Engineering Fracture Mechanics*, Vol. 72, pp. 255-269.

Guagliano, M.; Sangirardi, M.; Vergani, L. (2006): Photoelastic methods to determine K_I, K_{II} and K_{III} of internal cracks subjected to mixed mode loading. *Int. J. Fatigue*, Vol. 28, pp. 576-582.

Kassir, M.K.; Sih, G.C. (1966): Three-dimensional stress distribution around an elliptical crack under arbitrary loadings. *ASME J. Appl. Mech*, vol. 33, pp. 601-611.

Paris, F.; Picon, R.; Marin, J.; Cañas, J. (1997): Photoelastic determination of K_I and K_{II}: a numerical study on experimental data. *Exp. Mech.*, vol. 37, pp. 45-56.

Smith, C.W.; Olaosebikan, O. (1984): Use of mixed-mode stress-intensity algorithms for photoelastic data. *Exp. Mech*, vol. 24, pp. 300-307.

Smith, C.W.; Post, D.; Nicoletto, G. (1983): Experimental stress-intensity distributions in three-dimensional cracked-body problems. *Exp. Mech*,

vol. 23, pp. 378-382.

Zhengmei, L.; Ping, S. (1983): Photoelastic determination of mixed-mode stress-intensity factors K_I, K_{II} and K_{III}. *Exp. Mech.*, vol.23, pp. 228-235.